In vivo roles for Arp2/3 in cortical actin organization during *C. elegans* gastrulation

Minna Roh-Johnson and Bob Goldstein

Biology Department, University of North Carolina at Chapel Hill, Chapel Hill, NC 27599, USA
minna_roh@med.unc.edu; bobg@unc.edu

Accepted 19 August 2009
Journal of Cell Science 122, 3983-3993 Published by The Company of Biologists 2009
doi:10.1242/jcs.057562

Summary

The Arp2/3 complex is important for morphogenesis in various developmental systems, but specific in vivo roles for this complex in cells that move during morphogenesis are not well understood. We have examined cellular roles for Arp2/3 in the *Caenorhabditis elegans* embryo. In *C. elegans*, the first morphogenetic movement, gastrulation, is initiated by the internalization of two endodermal precursor cells. These cells undergo a myosin-dependent apical constriction, pulling a ring of six neighboring cells into a gap left behind on the ventral surface of the embryo. In agreement with a previous report, we found that in Arp2/3-depleted *C. elegans* embryos, membrane blebs form and the endodermal precursor cells fail to fully internalize. We show that these cells are normal with respect to several key requirements for gastrulation: cell cycle timing, cell fate, apicobasal cell polarity and apical accumulation and activation of myosin-II. To further understand the function of Arp2/3 in gastrulation, we examined F-actin dynamics in wild-type embryos. We found that three of the six neighboring cells extend short, dynamic F-actin-rich processes at their apical borders with the internalizing cells. These processes failed to form in embryos that were depleted of Arp2/3 or the apical protein PAR-3. Our results identify an in vivo role for Arp2/3 in the formation of subcellular structures during morphogenesis. The results also suggest a new layer to the model of *C. elegans* gastrulation: in addition to apical constriction, internalization of the endoderm might involve dynamic Arp2/3-dependent F-actin-rich extensions on one side of a ring of cells.

Supplementary material available online at
http://jcs.biologists.org/cgi/content/full/122/21/3983/DC1

Key words: Arp2/3, F-actin, Gastrulation, Morphogenesis, *C. elegans*

Introduction

Morphogenesis involves the reorganization of cells by cell shape changes and cell movements, both of which require intricate regulation of cytoskeletal dynamics. Some of the central goals of studying morphogenesis are to understand how cytoskeletal dynamics are regulated and how the reorganization of the cytoskeleton drives the movements of cells during development.

Gastrulation is one of the first morphogenetic movements in animal embryos. In most embryos, the three germ layers – ectoderm, mesoderm and endoderm – become positioned during gastrulation. Gastrulation in *Caenorhabditis elegans* is a powerful model system for dissecting mechanisms of morphogenesis because it involves a small number of cells and hence can be studied at the level of individual cells. Also, one can readily combine live microscopic imaging with gene function studies. Gastrulation in *C. elegans* is initiated at the 26-cell stage by the internalization of the anterior and posterior endodermal precursor cells, Ea and Ep (referred to collectively as Ea/p). Normal cell fate is required for Ea/p cell internalization: mutations in endoderm-specifying genes, such as the endodermal GATA factor genes *end-1* and *end-3*, result in gastrulation defects (Zhu et al., 1997; Maduro et al., 2005; Lee et al., 2006). Ectopic endodermal cells produced experimentally by cell fate transformation also internalize (Lee et al., 2006). As the Ea/p cells internalize in wild-type embryos, a ring of six cells fills a gap left behind on the ventral surface of the embryo (Lee and Goldstein, 2003). After the Ea/p cells internalize, they divide in the center of the embryo and eventually form the entire endoderm.

The Ea/p cells move to the embryonic interior in part through apical constriction. The Ea/p cells apically accumulate non-muscle myosin-II (NMY-2) (Nance and Priess, 2002). This polarized accumulation requires the PAR proteins (Nance and Priess, 2002), which are conserved polarity proteins with homologs in *Drosophila* and vertebrates (Goldstein and Macara, 2007). Certain PAR proteins such as PAR-3, PAR-6 and an atypical protein kinase C, localize to the apical surfaces of the Ea/p cells, whereas PAR-1 and PAR-2 are basolaterally localized (Etemad-Moghadam et al., 1995; Boyd et al., 1996; Hung and Kemphues, 1999; Nance and Priess, 2002). Myosin-II becomes activated in a Wnt-dependent manner by phosphorylation of the regulatory myosin light chains (rMLC) (Lee et al., 2006). This activation results in a contraction of the actomyosin meshwork in the apical cell cortex of each Ea/p cell, which is thought to pull the ring of neighboring cells underneath, driving the Ea/p cells to the interior of the embryo.

The known roles for actin in Ea/p cell movements suggest that actin regulation might be involved in this process. One major regulator of the actin cytoskeleton is the Arp2/3 complex (Vartiainen and Machesky, 2004). This complex is composed of seven subunits that act together to nucleate new actin filaments off of pre-existing actin filaments (Pollard, 2007). Two subunits of the Arp2/3 complex are actin-related proteins that nucleate growth of the new filament, and the other five proteins link the two actin-related proteins to the mother filament (Rouiller et al., 2008). In cultured motile cells, where roles for Arp2/3 are intensively studied, Arp2/3-dependent branching at the leading edge results in a densely interconnected network of F-actin that functions to push the membrane forward,

producing a pseudopod (Pollard, 2007). The interaction of the Arp2/3 complex with nucleation-promoting factors, such as the WASp/Scar family of proteins, stimulates the formation of new branched actin filaments, further pushing the membrane forward for cell migration (Pollard and Borisy, 2003).

Loss-of-function studies in diverse whole organisms have revealed that Arp2/3 is important for a variety of functions that involve the actin cytoskeleton (Vartiainen and Machesky, 2004). Arp2/3 is important for endocytosis in yeast and phagocytosis in mammals (May et al., 2000; Warren et al., 2002). Given the well established role of Arp2/3 in regulating actin dynamics, it is perhaps not surprising that Arp2/3 regulates the shaping of specialized actin-based structures in developing systems. Studies in *Drosophila* have shown a role for Arp2/3 in ring canal morphogenesis: Arp2/3 affects the size of the ring canal during oogenesis (Hudson and Cooley, 2002; Somogyi and Rorth, 2004). Myoblast fusion and pseudocleavage furrow formation are also regulated by Arp2/3 (Stevenson et al., 2002; Massarwa et al., 2007). Recently, it has been found that the role of Arp2/3 in endocytosis affects the remodeling of epithelial adherens junctions (Georgiou et al., 2008). Many studies have also identified roles for Arp2/3 and its upstream regulators in shaping plant cells (Mathur, 2005). These studies from metazoa, fungi and plants have revealed roles for Arp2/3 in non-motile cells, much less is known about how Arp2/3 functions in the embryonic cells that move during morphogenetic events.

Depleting *C. elegans* of Arp2/3 subunits resulted in bleb-like extensions on cells and gastrulation defects: Ea/p cells fail to move to the embryonic interior and instead divide on the surface of the embryo (Severson et al., 2002). *C. elegans* Arp2/3-encoding genes are named Arp2/3-related complex or *arx* genes (Sawa et al., 2003; Severson et al., 2002). *arx-2* and *arx-1* encode the Arp2 and Arp3 homologues, respectively. Depleting *C. elegans* Arp2/3 subunits by RNAi results in more than 95% embryonic lethality (Severson et al., 2002). Arp2/3 RNAi embryos also have defects in ventral enclosure, a process in which the embryonic epidermis migrates from the dorsal surface and seals the ventral surface (Severson et al., 2002; Sawa et al., 2003; Patel et al., 2008). In Arp2/3-depleted embryos, the leading edge of the migrating epidermis lacks a normal enrichment of filamentous actin, and finger-like protrusions that normally form are absent (Sawa et al., 2003). Another role for Arp2/3 was found in migrating excretory cells in *C. elegans*, where Arp2/3 was discovered to be involved in longitudinal migration (Schmidt et al., 2009). To our knowledge, no other reports have dissected roles for the Arp2/3 complex in cells that move during morphogenesis in animal embryos. Furthermore, there are very few studies examining the roles of Arp2/3 in the moving cells of intact animals as the movements are taking place. Exploring such roles is an important step toward understanding the breadth of in vivo functions of this complex.

To determine cellular roles for the Arp2/3 complex in the embryonic cells that move during morphogenetic events, we used a combination of live imaging and immunohistochemistry in wild-type and siRNA-treated *C. elegans* embryos. A number of possible roles were suggested by the known direct functions of Arp2/3 in F-actin nucleation and branching, as well as by indirect roles for Arp2/3 in endocytosis, apicobasal protein targeting, adhesion and cell motility (Kovacs and Yap, 2002; Guerriero et al., 2006; Le Clainche and Carlier, 2008; Galletta and Cooper, 2009). We report that Arp2/3 is enriched at the cell cortex, and that previously observed membrane protrusions (Severson et al., 2002) that form in Arp2/3 RNAi embryos are classical membrane blebs. Despite the blebs observed in Arp2/3-depleted embryos, the cells that would normally participate in gastrulation appeared normal with respect to several key upstream inputs to gastrulation: cell-cycle timing, cell fates, apicobasal cell polarity, and apical accumulation and activation of myosin-II. To further explore how Arp2/3 might affect gastrulation, we examined F-actin dynamics in living wild-type embryos during gastrulation. We found that dynamic F-actin-rich structures form on specific cells – cells on one side of the ring of cells that fills the gap left by the internalizing Ea/p cells, at their apical boundaries with the Ea/p cells. These F-actin-rich structures failed to form in embryos that were depleted of Arp2/3 or the apical protein PAR-3. Our results identify an in vivo role for Arp2/3 during morphogenetic cell movements. The results also suggest that internalization of the endoderm in *C. elegans* involves dynamic Arp2/3-dependent F-actin-rich extensions that form on specific cells.

Results

Arp2/3 depletion results in partial shrinking of the Ea/p apical surfaces and incomplete Ea/p cell internalization

Severson and co-workers (Severson et al., 2002) reported that depletion of Arp2/3 complex members by RNAi resulted in dead embryos and found that the Ea and Ep cells failed to internalize. We began by confirming this result. In wild-type embryos, Ea and Ep were borne on the surface of the embryo and moved to the interior before dividing (Fig. 1A-D). In Arp2/3-depleted embryos, Ea and Ep failed to completely internalize, and divided on the surface of the embryo (Fig. 1E-H). The gastrulation defects in embryos depleted of *arx-1* (n=65) or *arx-2* (n=25) by RNAi were both 100% penetrant. In subsequent experiments depleting Arp2/3, we depleted embryos of either *arx-1* or *arx-2* by injecting double-stranded RNA into the parental strain, because either resulted in gastrulation defects at high penetrance. For convenience we refer to either treatment as Arp2/3 RNAi.

To understand why endodermal internalization did not complete in Arp2/3-depleted embryos, we further quantified the degree to which cell internalization failed by placing embryos on their lateral sides and measuring the maximum anterior-to-posterior length of the exposed surfaces of Ea and Ep. In wild-type embryos, these exposed apical lengths decreased over time, and by 14 minutes after neighboring MS cells (MSa/p) divided, the apical surfaces of Ea and Ep were covered or almost entirely covered by neighboring cells (Fig. 1I). In Arp2/3 RNAi embryos, the lengths of exposed apical Ea/p cell surfaces began to decrease as in the wild type, but this process failed to complete (Fig. 1J). To visualize the entire apical surface as Ea/p cell internalization occurred, we imaged the cell-cell boundaries on the ventral surface of embryos using a plasma membrane marker, a fluorescently tagged pleckstrin-homology domain of phospholipase C gamma (PH::mCherry) (Kachur et al., 2008). We traced the apical edges of an Ep cell as the exposed surface decreased in total area (Fig. 1K). Tracing apical edges in an Arp2/3-depleted embryo showed, as with the lateral measurements, that the apical surface failed to fully decrease in size (Fig. 1K). We conclude that in Arp2/3-depleted embryos, the Ea/p cells began to internalize, and they failed to completely move to the interior of the embryo, leaving much of their apical surfaces exposed to the exterior of the embryo.

Arp2/3 is enriched at the cell cortex and is required for stable membrane-cytoskeletal linkages

Before examining specific functions of Arp2/3 in gastrulation, we explored its general functions in cells of the early *C. elegans*

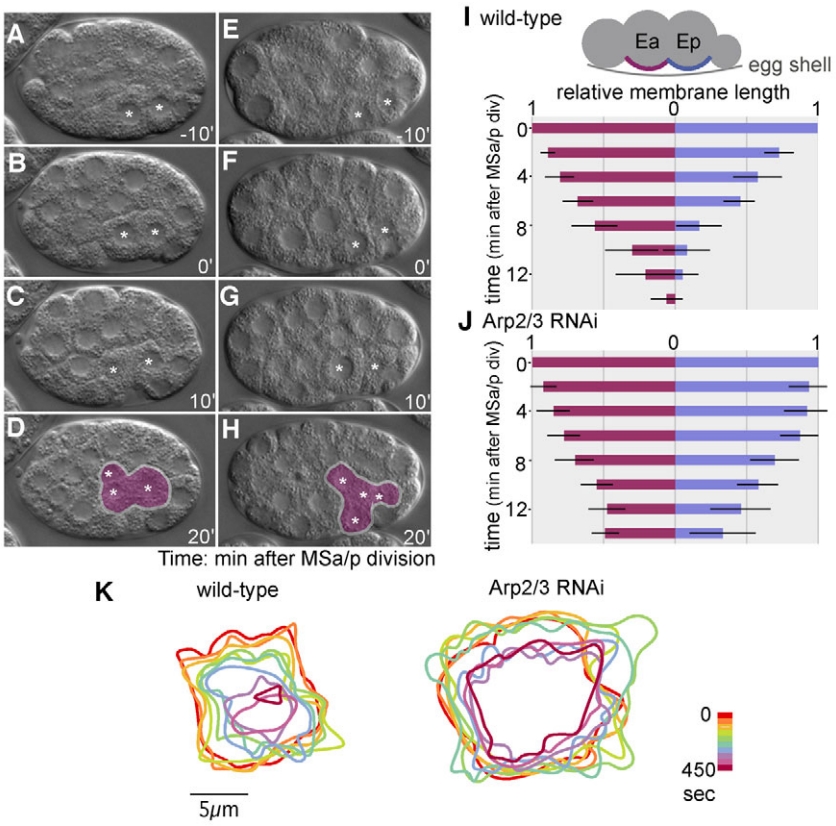

Fig. 1. Arp2/3 depletion results in only partial shrinking of the Ea/p cell apical surfaces. (A-D) The Ea/p cells move into the interior of the embryo as surrounding cells fill in the gap left in the ventral (bottom) side. The Ea/p cells subsequently divide (D) in the interior. Only three of the four Ea/p descendants (shaded in purple) are marked with asterisks because the fourth descendant is not in same imaging plane. (E-H) Ea/p cells in Arp2/3-depleted embryos begin to move to the interior but fail to complete internalization and divide on the surface of the embryo. The progeny of Ea/p did eventually internalize as four cells. In this and subsequent figures, asterisks indicate Ea/p cells and/or Ea/p descendants, except where noted. (I) Lengths of exposed Ea/p apical surfaces are shown as ratios of the initial lengths ±95% confidence intervals. In wild-type embryos (n=6), Ea/p cells internalized by ~14 minutes after MSa/p division. (J) In Arp2/3 RNAi embryos (n=6), the lengths of exposed apical Ea/p cell surfaces failed to completely decrease to zero. (K) Tracings of en face (ventral) views of individual cells. The apical surfaces of Ea/p cells in wild-type and Arp2/3 RNAi embryos were traced at 50 second intervals from films of the PH:mCherry membrane marker, and individual tracings were color-coded by time and overlaid. The colored scale indicates seconds after MSa/p division.

embryo by examining its localization and loss-of-function phenotype in early embryos. The Arp2/3 complex localizes to branched actin at the leading edge of migrating cells and in the cell cortex in other systems (Mullins et al., 1997; Svitkina and Borisy, 1999). However, antibodies previously generated against *C. elegans* ARX-1 (Arp3) and ARX-7 (ArpC5) showed only diffuse localization throughout the cytoplasm in embryos (Sawa et al., 2003). We generated affinity-purified polyclonal antibodies against ARX-5, the *C. elegans* homolog of ArpC3, which is the 21 kDa subunit. We immunostained embryos and found enrichment of ARX-5 near plasma membranes, consistent with the expected localization to the cell cortex (Fig. 2A-F). This pattern was seen at gastrulation and earlier, and it was eliminated using RNAi targeting *arx-5*. At the time of Ea/p cell internalization, ARX-5 was also present at sites where MS granddaughter cells contact Ea at the apical surfaces of the cells (Fig. 2C,E), sites that we discuss further below. We also saw diffuse cytoplasmic and P-granule staining, but RNAi targeting *arx-5* eliminated only the cortical signal, suggesting that the cytoplasmic and P-granule staining were primarily non-specific background. We conclude that, as expected given its known functions, Arp2/3 is enriched at the cell cortex at gastrulation and earlier.

In Arp2/3 RNAi embryos, cells formed membrane protrusions that were previously referred to as blebs (Severson et al., 2002). Blebbing involves detachment of the plasma membrane from the cortical cytoskeleton (Cunningham, 1995), but it is unclear whether the structures described previously reflect such detachments, as they were observed only by DIC microscopy (Severson et al., 2002). Once the membrane-cytoskeleton linkage is broken, blebs continue to expand. F-actin and other components of the contractile cortex then reassemble under the bleb membrane,

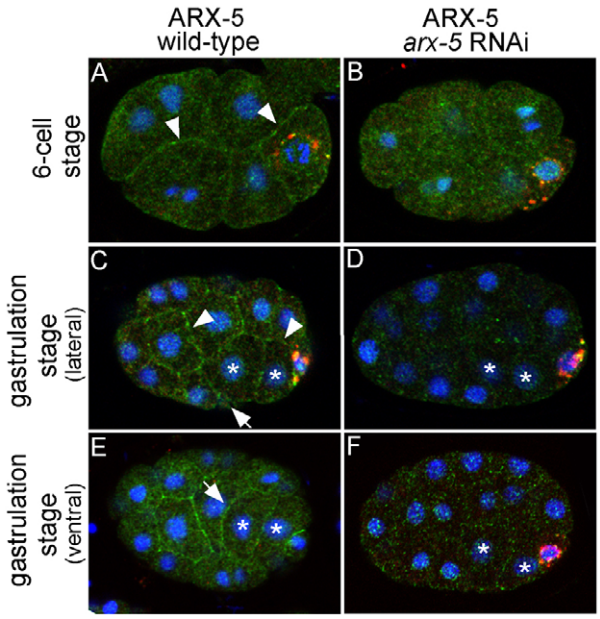

Fig. 2. The Arp2/3 complex is enriched near cell membranes. (A-F) Embryos immunostained with ARX-5 antibodies (green). (A,B) Embryos at the 6- to 8-cell stage. ARX-5 appears enriched near plasma membranes (arrowheads). In control *arx-5* RNAi embryos, enrichment near plasma membranes is reduced or absent. (C-F) Lateral views (C,D) and ventral views (E,F) of gastrulation-stage embryos also revealed ARX-5 localization near membranes (arrowheads). ARX-5 was similarly enriched at borders between MSxx and Ea cells (arrow). Cortical staining was absent in *arx-5* RNAi embryos. Antibodies to P-granules were used to confirm permeabilization of embryos to immunostaining reagents (red). Nuclei are stained with DAPI (blue).

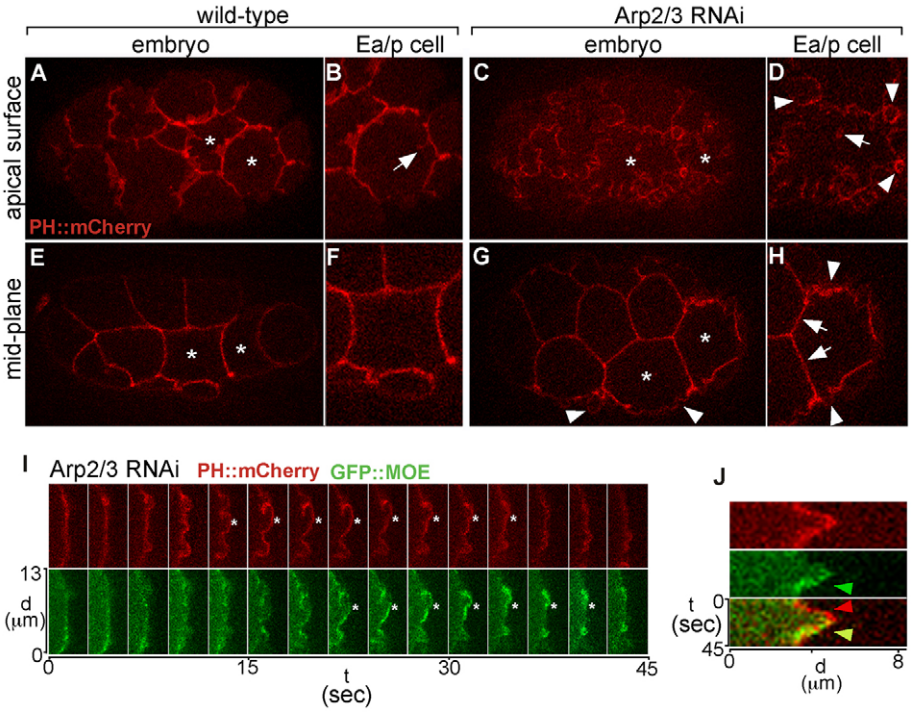

Fig. 3. Arp2/3 is required for stable membrane-cytoskeletal linkages at free cell surfaces. (A-H) Ventral views of embryos expressing PH::mCherry plasma membrane marker. (A) A surface view of a wild-type embryo. (B) A higher magnification of the Ep cell. The arrow indicates an apparent membrane tether. (C) A surface view of an Arp2/3 RNAi embryo. (D) A higher magnification of the Ea cell with blebs (arrowheads) and apparent infolding of the surface in the center of the cell (arrow). (E) A mid-plane view of a wild-type embryo. (F) A higher magnification of the Ea cell. (G) A mid-plane view of an Arp2/3 RNAi embryo. Blebs (arrowheads) formed at free apical surfaces. (H) A higher magnification of the Ep cell. Membranes at cell-cell contacts appeared normal (arrows). Blebs (arrowheads) formed only at free apical surfaces (n=37 embryos). (I) Images of an embryo expressing GFP::MOE and PH:mCherry. For PH::mCherry, asterisks indicate the membrane bleb. For GFP::MOE, asterisks indicate when F-actin accumulated beneath the bleb. (J) A 45-second kymograph of the images in I, showing individual markers and both markers merged. GFP::MOE is not enriched under the plasma membrane during bleb formation (red arrowhead). GFP::MOE then appears enriched near the plasma membrane (green arrowhead) and the membrane retracts (yellow arrowhead).

and the bleb retracts (Charras et al., 2006). To determine whether Arp2/3 is required for such membrane-cytoskeletal linkage, we first examined the protrusions of Arp2/3-depleted embryonic cells using the plasma membrane marker PH::mCherry. These protrusions formed throughout embryogenesis. Arp2/3-depleted embryos appeared to form membrane protrusions on all of the external cell surfaces (Fig. 3C,D), whereas wild-type embryos formed only flattened membrane extensions and apparent membrane tethers (Fig. 3A,B). When we examined the mid-plane of Arp2/3-depleted embryos, we found that the rounded protrusions only formed at the contact-free surfaces (Fig. 3G,H) and not at surfaces that were in contact with other cells (Fig. 3C,D,G,H). Next, to simultaneously image plasma membranes and underlying F-actin dynamics, we crossed the PH::mCherry membrane marker into a strain expressing a GFP-tagged F-actin-binding domain from *Drosophila* moesin (GFP::MOE), which has been used in *Drosophila* and *C. elegans* to specifically mark the filamentous form of actin (Edwards et al., 1997; Motegi et al., 2006). In Arp2/3 RNAi embryos, the apical membrane formed rounded protrusions that lacked cortical GFP::MOE enrichment under the bleb membrane as the bleb expanded (Fig. 3I). Once the bleb stopped expanding, GFP::MOE accumulated under the bleb membrane, and the bleb retracted (n=21/21 blebs) (Fig. 3I,J; supplementary material Movie 1). Therefore, the cellular protrusions observed in Arp2/3 RNAi embryos have characteristics that suggest that they are true membrane blebs. Consistent with the lack of cytoskeletal support observed under growing blebs, we did not observe blebs after fixation and processing for immunostaining (see later results). We conclude that Arp2/3 is important in this system for the membrane-cytoskeletal linkages that normally prevent blebbing, possibly through an effect on actin cytoskeletal integrity. Despite the formation of membrane blebs, cell divisions still occurred, and the first developmental defect that we and others observed was failure of Ea/p cell internalization. Therefore, to determine the cellular mechanisms underlying this gastrulation defect, we examined several key factors that regulate Ea/p cell internalization.

Arp2/3-depleted embryos have normal cell fates during gastrulation

Actin-based intracellular motility is important in cell-fate specification (Takizawa et al., 1997) and failure to specify endodermal cell fate can prevent gastrulation (Lee et al., 2006). Therefore, we speculated that defective cell-fate specification could underlie the gastrulation defect of Arp2/3-depleted embryos. Severson and colleagues (Severson et al., 2002) reported that terminally arrested Arp2/3 RNAi embryos produced some endoderm, but whether this fate was established on time and in the appropriate cells was not examined. We analyzed the expression patterns of two fate markers that are expressed as gastrulation occurs: *end-1::*GFP, a marker for endodermal fate (Calvo et al., 2001), and *ceh-51::*GFP, a marker for MS lineage fate (Broitman-Maduro et al., 2009). In Arp2/3 RNAi embryos, *end-1::*GFP was expressed in the E lineage, similarly to expression in wild-type embryos (supplementary material Fig. S1A,B). Likewise, we observed *ceh-51::*GFP expression specifically in MS progeny when Arp2/3 function was knocked down (supplementary material Fig. S1D,E). These results suggest that loss of Arp2/3 does not prevent timely E or MS cell fate specification.

One aspect of normal Ea/p cell fate is the introduction of a G2 phase to the cell cycle in Ea and Ep, delaying division of these cells until they become internalized (Edgar and McGhee, 1988). Because there is evidence that premature division of the Ea/p cells can prevent their internalization (Lee et al., 2006), we examined cell-cycle timing after Arp2/3 depletion, measuring the time between Ea/p birth and Ea/p division. In wild-type embryos, Ea/p divided 43.6±4.3 (mean ± s.d.) minutes after they were born (n=9). In Arp2/3-depleted embryos, Ea/p divided 49.2±3.4 minutes after they were born (n=16). Therefore, Ea/p cells did not divide prematurely in Arp2/3-depleted embryos.

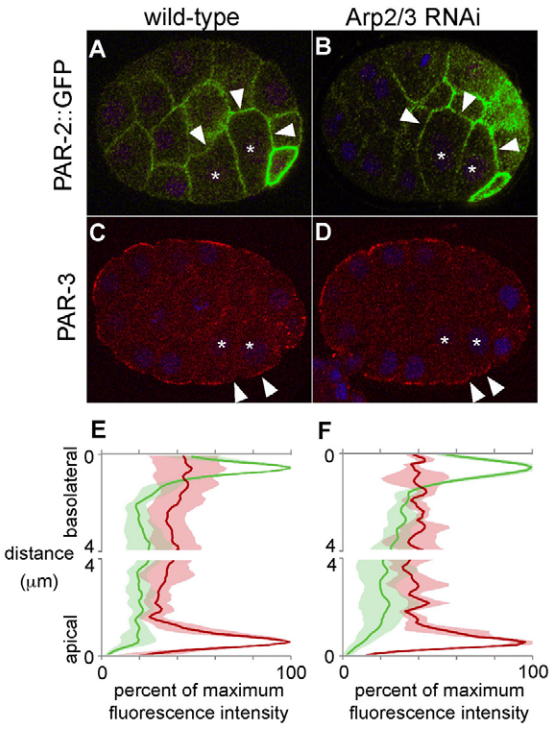

Fig. 4. Arp2/3-depleted embryos localize apical PAR-3 and basolateral PAR-2 proteins normally. (A,B) Fixed embryos at gastrulation stage immunostained for PAR-2::GFP. In wild-type (*n*=12/12) and in Arp2/3 RNAi embryos (*n*=12/12), PAR-2::GFP localized basolaterally (arrowheads). (C,D) Wild-type embryos (*n*=7) and Arp2/3 RNAi embryos (*n*=6/6) immunostained for endogenous PAR-3 showed apical accumulation in all cells, including Ea/p (arrowheads). (E) anti-PAR-3 (red, *n*=7) and PAR-2::GFP (green, *n*=6) fluorescence intensity levels quantified in wild-type and Arp2/3 RNAi Ea/p cells show peaks of fluorescence intensity at the apical and basolateral membrane, respectively. Shading indicates 95% confidence intervals.

Arp2/3-depleted embryos exhibit normal apicobasal polarity

Ea/p cells are apicobasally polarized, with PAR-3 and PAR-6 enriched near apical surfaces and PAR-2 enriched near basolateral membranes (Etemad-Moghadam et al., 1995; Boyd et al., 1996; Hung and Kemphues, 1999; Nance and Priess, 2002). When PAR proteins are experimentally degraded in somatic cells before gastrulation, the Ea/p cells have internalization defects (Nance et al., 2003). The Arp2/3 complex has been implicated in vesicle trafficking (Fucini et al., 2002; Luna et al., 2002), which could affect apicobasal polarity and PAR protein localization. To determine whether cells in Arp2/3-depleted embryos were properly polarized, we examined the localization of PAR proteins. In Arp2/3 RNAi embryos, PAR-2::GFP localization was indistinguishable from that in the wild type (Fig. 4A,B). When we examined the localization of the endogenous apical PAR protein PAR-3, we found that PAR-3 accumulated near the apical cell membranes of Arp2/3 RNAi embryos similarly to its accumulation in wild-type embryos (Fig. 4C,D). Quantification of fluorescence levels across cells confirmed that protein localization profiles in the wild type and Arp2/3 RNAi embryos were similar (Fig. 4E). Apicobasal polarization of these PAR proteins in other cells also appeared normal (Fig. 4A-D). We conclude that the Arp2/3 complex is not required for apicobasal polarization of PAR protein distributions.

Apical accumulation and activation of myosin are normal in Arp2/3-depleted embryos

Apicobasally polarized Ea/p cells accumulate the tagged myosin heavy chain NMY-2::GFP at their apical surfaces (Nance and Priess,

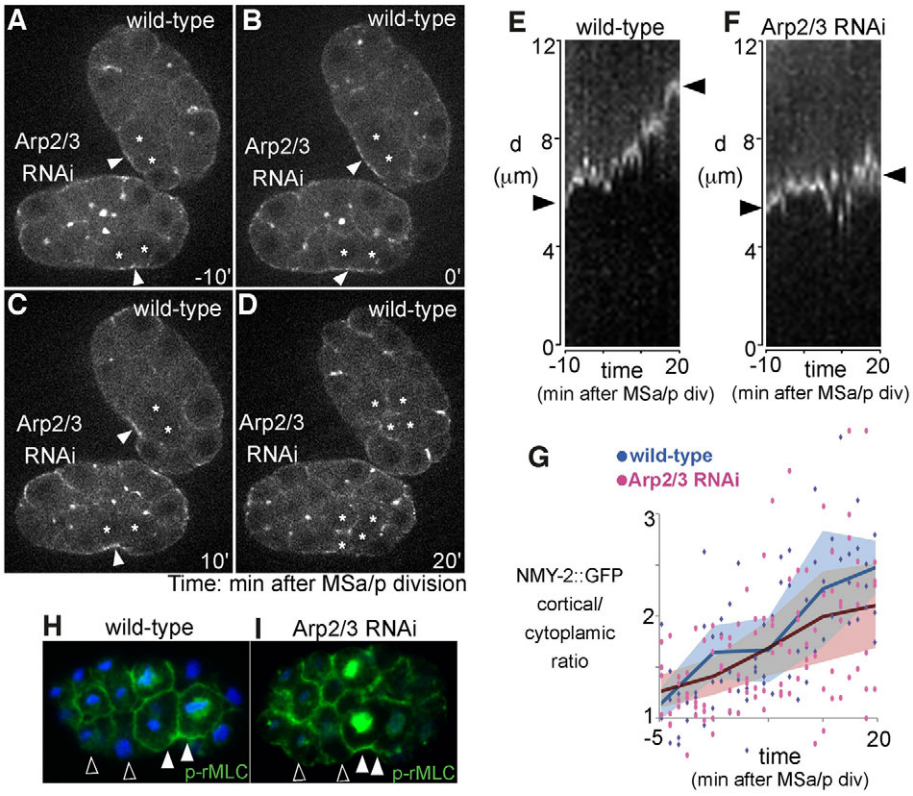

Fig. 5. Apical accumulation and activation of myosin is normal in Arp2/3-depleted embryos. (A-D) Wild-type and Arp2/3-depleted NMY-2::GFP embryos of the same age placed side-by-side show apical myosin accumulation (arrowheads). Arp2/3 RNAi embryos accumulated NMY-2::GFP apically in Ea/p (*n*=21/21 embryos). (E,F) Kymographs of the same embryos over 30 minutes. Arrowheads at the sides of the kymograph indicate the initial and final position of the NMY-2::GFP-enriched apical cortex. d, distance in μm from an arbitrary point. (G) Graph of cortical to cytoplasmic ratios of NMY-2::GFP fluorescence intensities over time in wild-type and Arp2/3 RNAi embryos. All measurements from wild-type (*n*=3) and Arp2/3 RNAi embryos (*n*=4) were plotted and lines that represent the averages of 5 minute intervals were drawn. Shaded regions indicate 95% confidence intervals. (H,I) Wild-type embryos stained with rMLC-*P* (p-rMLC) antibody shows apical distribution in Ea/p-enriched cells (white arrowheads) compared with neighboring cells (black arrowheads) in both wild-type and Arp2/3 RNAi embryos. Nuclear staining is a background signal (Lee et al., 2006).

2002). We examined NMY-2::GFP-expressing embryos (Nance et al., 2003) to determine whether apical myosin accumulation is affected in Arp2/3-depleted embryos. Wild-type NMY-2::GFP and Arp2/3 (RNAi); NMY-2::GFP embryos at the same stage were recorded side-by-side to facilitate quantification of protein levels in parallel (Fig. 5). In both wild-type and Arp2/3-depleted embryos, NMY-2::GFP accumulated apically 10 minutes before MSa/p division (Fig. 5A). As the apical surface profiles of the Ea/p cells decreased in length, the apical myosin accumulation could still be seen (Fig. 5B,C). In Arp2/3 RNAi embryos, NMY-2::GFP was still enriched apically in the Ea/p cells, and the Ea/p cells failed to internalize and instead divided on the surface of the embryo (Fig. 5D). Kymographs of wild-type embryos confirmed that NMY-2::GFP was enriched on the apical surface of the Ea/p cells as this surface moved toward the interior of the embryo (Fig. 5E). In Arp2/3 RNAi embryos, NMY-2::GFP was enriched similarly near the apical surface because this surface failed to move toward the interior of the embryo (Fig. 5F). We quantified cortical NMY-2::GFP levels and found that the cortical-to-central fluorescence intensity ratios rose as expected over time, and were statistically indistinguishable between wild-type and Arp2/3-depleted embryos (Fig. 5G). We conclude that apical myosin accumulates normally in Ea/p cells in Arp2/3-depleted embryos.

The apically localized myosin in the Ea/p cells becomes activated by Wnt-dependent regulatory light chain phosphorylation as cell internalization begins (Lee et al., 2006). To determine whether Arp2/3 is required to activate myosin-II, wild-type and Arp2/3 RNAi embryos were immunostained with an antibody that recognizes the activated (serine-phosphorylated) form of myosin regulatory light chain (rMLC-*P*). We found that in Arp2/3 RNAi embryos, rMLC-*P* accumulated on the apical surfaces of the Ea/p cells more so than in other cells, as in the wild type (Fig. 5H). These results suggest that apical myosin in Ea/p is activated normally in Arp2/3-depleted embryos.

Three of the six cells surrounding the Ea/p cells form dynamic F-actin-rich structures

Because gastrulation failed in Arp2/3 embryos despite normal cell fates, cell-cycle timings and cell polarity, and with myosin localized and activated normally, we pursued other possible roles for Arp2/3 during gastrulation. Phalloidin staining of fixed, wild-type embryos has not identified any specialized F-actin-rich structures such as filopodia or lamellipodia during gastrulation (Lee and Goldstein, 2003), but it is possible that fixation artifacts could have eliminated such structures. Therefore, we examined F-actin organization in living, wild-type embryos using GFP::MOE. As part of this analysis, embryos were placed on their ventral sides to image the ring of cells that fill the gap left by the internalizing Ea/p cells. This ring of cells is composed of three of the four MS cell granddaughters (MSpp, MSpa, MSap, but not MSaa), two AB descendants (usually ABplpa and ABplpp), and the single germline precursor cell (P_4). Mid-plane imaging was used to determine the location of the Ea/p cells and neighboring cells. We then imaged at the ventral surface of each embryo where the neighboring cells border the internalizing Ea/p cells. We found that specific cells formed dynamic F-actin-rich structures at their apical borders with the Ea/p cells (supplementary material Movie 2). Three of the six surrounding cells formed these structures, and tracing cell lineages revealed that these three cells were the three MS descendants that comprise half of the ring (Fig. 6A,B). These F-actin-rich structures formed in the same places where flattened structures had been reported previously in fixed embryos by scanning electron microscopy (Nance and Priess, 2002) on the apical sides of MS granddaughter cells, where they contacted internalizing Ea/p cells and not on other cells such as P_4 (Nance and Priess, 2002). For this reason, we now interpret the flattened processes first reported by Nance and Priess (Nance and Priess, 2002) as F-actin-rich processes, and we show below that these processes are dynamic in living embryos. The AB

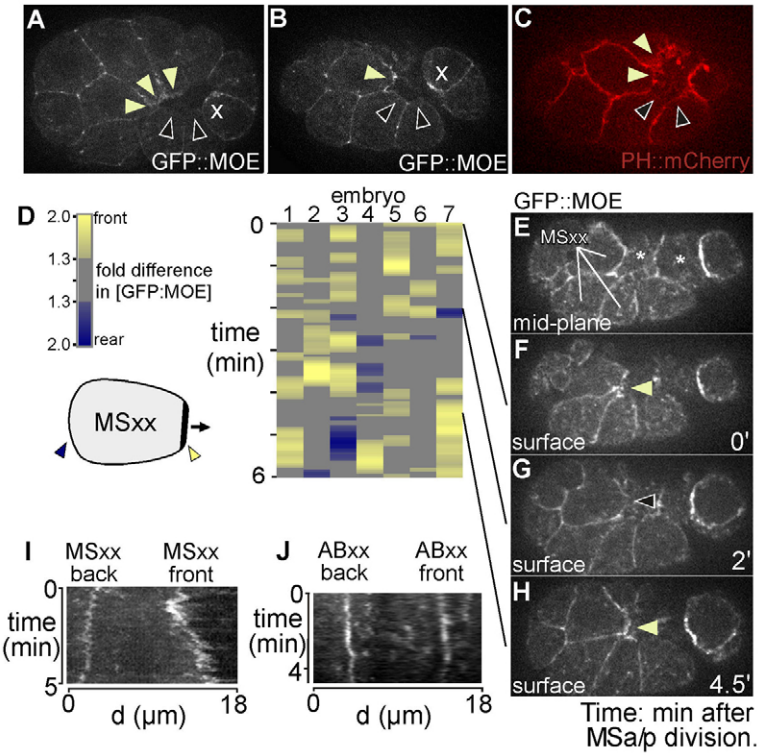

Fig. 6. Three of the six cells surrounding the Ea/p cells produce dynamic, F-actin-rich structures. (A-C) Embryos viewed from their ventral sides. (A,B) GFP::MOE-expressing embryos. F-actin-rich structures (yellow arrowheads) formed at the borders of the MS descendants and the Ea/p cells. The AB descendants, ABplpa and ABplpp, did not form these F-actin-rich structures at their borders with the Ea/p cells (black arrowheads). F-actin enrichment at the P_4/Ep cell boundary is marked by an 'x'. (C) An embryo expressing PH::mCherry showing F-actin-rich processes specifically at the borders of MS descendants and the Ea/p cells and not at the borders of AB descendants and the Ea/p cells. (D) Heatmap representing GFP::MOE accumulation in seven individual embryos. Yellow and blue colors indicate GFP::MOE front to back end ratios above 1.3-fold difference. Front and back ends are defined with respect to direction of extension across the gap as indicated in the diagram. The preponderance of yellow in the resulting heatmap indicates frequent enrichment of GFP::MOE at the front end. (E-H) Representative images from a wild-type GFP::MOE embryo, embryo 7 of the heatmap. (E) Mid-plane view. Ea/p cells are marked by asterisks and the three MSxx cells are labeled. (F-H) GFP::MOE accumulated at the border of MSxx and the Ea/p cells at certain times (yellow arrowhead) and not at other times (black arrowhead). We did not observe GFP::MOE accumulation at the back end of MSxx cells in the imaging plane shown, nor in other planes. (I) Kymograph of a line across an MSxx cell of a GFP::MOE expressing embryo. The front end of MSxx has dynamic enrichment of GFP::MOE. (J) Kymograph of a line across an ABxx cell of a GFP::MOE expressing embryo. The front end of ABxx does not have dynamic GFP::MOE enrichment.

descendants of the ring did not form similar F-actin-rich structures at their apical borders with the Ea/p cells (Fig. 6A,B). We found similar flattened membrane processes on MSpp, MSpa and MSap cells in PH::mCherry embryos (Fig. 6C). This and previous scanning electron microscopy (SEM) reports suggest that these processes are not artifacts of GFP::MOE expression.

We analyzed movies of GFP::MOE embryos to examine F-actin dynamics. F-actin accumulation at the apical sides of MS granddaughters (referred to as MSxx cells) where they contact Ea/p was highly dynamic, with enrichment appearing and disappearing several times during Ea/p internalization (Fig. 6D-H). Kymographs of MOE::GFP in the MSxx cells confirmed F-actin enrichment and dynamic fluctuations of fluorescence intensity at the apical cell boundary with Ea/p cells (we refer to this as the front of the cell), and weaker and less dynamic F-actin localization at the rear MSxx cell boundary (Fig. 6I). The apical border between ABxx and Ea/p cells did not show similar F-actin enrichment (Fig. 6J). We conclude that MSxx cells are polarized with respect to F-actin localization and dynamics, unlike the AB progeny that comprise parts of the same ring.

F-actin-rich regions were also present on the P_4 cell where it contacted Ep (Fig. 6A-C). F-actin enrichment at the P_4-Ep border differs from that in MSxx cells in that it appears over multiple cell cycles at the borders between endodermal precursors and germline precursors, and it appears in a disc at the entire cell-cell contact region, rather than just at the apical side of this region (Goldstein, 2000).

The F-actin-rich extensions are dependent on the cell fate specification gene *pop-1*

Because F-actin-rich extensions formed specifically on MS granddaughter cells, and not on the other cells of the closing ring, we questioned whether the formation of these structures was dependent on MS cell fate. We transformed mesodermal cell fate using a *pop-1* mutant, in which MS cells are transformed into E cells (Lin et al., 1995). We confirmed the cell fate transformation by cell lineage analysis. In *pop-1* mutants, MSa/p cells divided with cell cycle timing that was similar to that of the Ea/p cells (supplementary material Fig. S2D,F). As the Ea/p cells internalized, the MS progeny also began to internalize (supplementary material Fig. S2F,G,J), and neighboring cells began to fill the gap left behind, although the gap was never completely filled (supplementary material Fig. S2J). We did not observe F-actin-rich structures where MS granddaughters contacted Ea/p cells, nor where neighboring cells contacted the internalizing MS cells (supplementary material Fig. S2L). We conclude that the formation of the F-actin-rich structures is dependent on the cell fate specification gene *pop-1*.

The F-actin-rich extensions that form on three MS granddaughter cells are Arp2/3- and PAR-3-dependent

Arp2/3 RNAi embryos have more convoluted membrane conformations specifically at their apical sides, where the plasma membrane bulges and detaches from the underlying cell cortex in blebs (Fig. 3). Thus, we predicted that Arp2/3 depletion might interfere with the apical enrichment of F-actin in MS progeny. We analyzed F-actin distribution using GFP::MOE in Arp2/3 RNAi embryos, and observed convoluted membrane conformations as before (Fig. 7A-E; supplementary material Movie 3). Additionally, we found that the MSxx-specific F-actin-rich structures did not form where these cells border Ea (Fig. 7B-D,F). Quantification of the front and back MSxx cell boundaries revealed that similar amounts

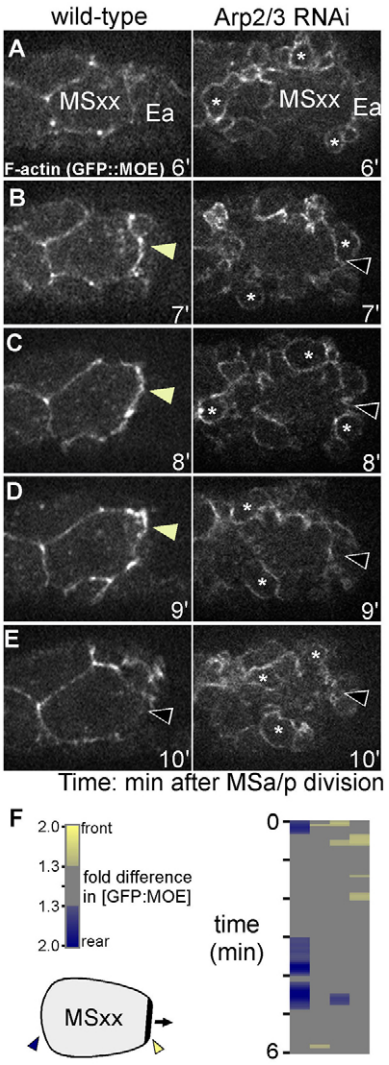

Fig. 7. The formation of the MSxx-specific F-actin-rich structures is Arp2/3 dependent. (A-E) Images from movies of wild-type and Arp2/3 RNAi embryos expressing GFP::MOE. Wild-type embryos formed F-actin-rich structures (yellow arrowheads), whereas Arp2/3 RNAi embryos cell membranes did not (black arrowheads) and instead formed membrane blebs (asterisks, *n*=6/6). (F) Quantification of GFP::MOE ratios at the front and back MSxx cell boundaries in four Arp2/3 RNAi embryos, with color-coded GFP::MOE ratios as in Fig. 6. The preponderance of gray indicates that ratios are frequently similar in Arp2/3 RNAi embryos.

of F-actin were frequently found at front and back ends of MSxx cells (Fig. 7F), unlike the more commonly polarized distribution we observed in the wild type. We conclude that Arp2/3 is required, directly or indirectly, for these F-actin-rich structures to form.

The polarized distribution of F-actin to processes in an apical region of the MSxx cells suggested that formation of these processes might depend on apicobasal polarization of MSxx cells. To test whether PAR-based cell polarization is required for formation of the MSxx processes, we crossed GFP::MOE into *par-3 ZF1*, a *C. elegans* strain in which the apical protein PAR-3 becomes degraded in somatic cells after the one-cell stage (Nance et al., 2003). We found that the MS-specific F-actin-rich structures did not form (Fig. 8A-F). Instead, the front and back MSxx cell boundaries appeared indistinguishable, each side with varying levels of GFP::MOE and

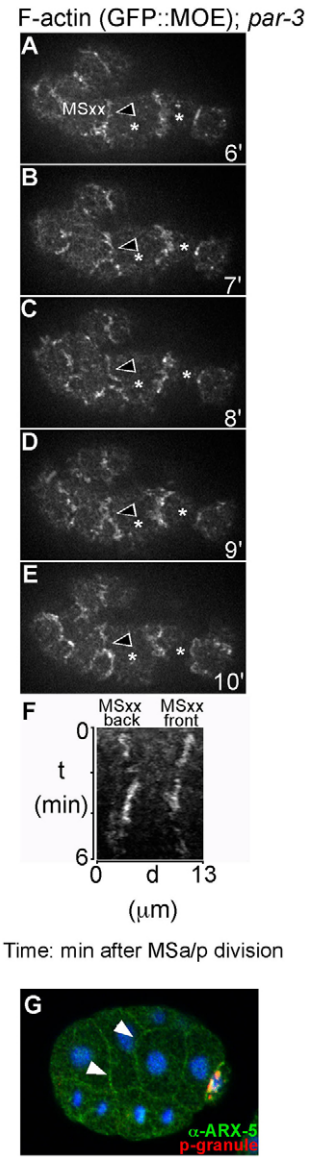

Fig. 8. The formation of MS-specific F-actin-rich structures requires the apical PAR protein PAR-3. (A-E) Images from a movie of *par-3 ZF1*; GFP::MOE. An MSxx cell is labeled, and the Ea/p cells are labeled with asterisks. Ea/p cells remained in the plane of imaging as expected from an internalization defect reported in *par-3* mutant embryos (Nance and Priess, 2002). Arrowheads indicate a boundary between MSxx and Ea cells. F-actin-rich structures did not form here in *par-3 ZF1* (n=7/7). (F) Kymograph of a line across MSxx. The kymograph shows that the MSxx front cell boundary did not transiently accumulate GFP::MOE above levels seen at the back end. (G) Cortical ARX-5 localization (arrowheads) in a *par-3 ZF1* mutant embryo.

without the apparent front end enrichment we observed in wild-type embryos. Analysis of ARX-5 localization in *par-3 ZF1* mutants revealed that ARX-5 localization was normal, suggesting, as expected, that PAR-3-dependent cell polarity is not required for Arp2/3 cortical localization (Fig. 8G). We conclude that PAR-3 is required to form F-actin-rich structures on the apical sides of MSxx cells where they border the Ea/p cells. Together, these results indicate that the dynamic, F-actin-rich structures depend directly or indirectly on Arp2/3 for their formation, as well as on cell polarity and cell fate proteins.

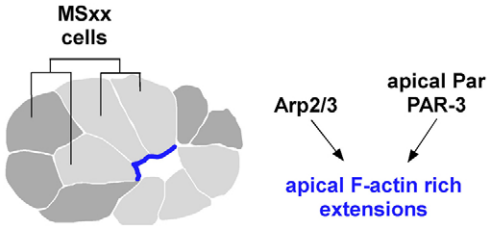

Fig. 9. Dynamic, MSxx-specific, F-actin-rich extensions require Arp2/3 and apical PAR protein. Six cells converge in a ring (light gray), filling in the space left by the internalizing E cells (white gap in middle). Three of these cells are MS descendants. F-actin-rich structures formed in MSxx cells that contacted Ea/p cells, at their apical sites of contact (blue). These structures were absent in embryos deficient in either Arp2/3 or the apical marker *par-3*.

Discussion

We have found that wild-type embryos form dynamic F-actin-rich structures specifically on mesodermal precursor cells during Ea/p cell internalization. These structures form transiently at the apical borders of MSap, MSpa and MSpp where they contact the internalizing Ea/p cells – sites consistent with where cell flattening had been seen previously by SEM (Nance and Priess, 2002) (Fig. 9). In Arp2/3-depleted embryos, cell fates, apicobasal cell polarity, myosin localization and myosin activation appeared normal, but plasma membrane association with the cell cortex was perturbed, and the F-actin-rich structures on MSxx cells were absent. Together with previous results (Severson et al., 2002), we conclude that Arp2/3 is required for completion of endoderm internalization in *C. elegans*. We speculate that the F-actin-rich structures lost in Arp2/3-depleted embryos might contribute to completion of gastrulation. Below, we discuss this possibility and alternatives. We also discuss roles for such structures in other systems.

The F-actin-rich structures we observed might be specializations for cell crawling, although we have not been able to directly test this hypothesis. Cell surface labeling experiments during gastrulation suggest that these cells do not exhibit surface retrograde flow, as crawling cells often do (Lee and Goldstein, 2003). Furthermore, when MSxx cells were removed and reassociated with Ea/p cells in various orientations, MSxx cells still moved in a direction consistent with the hypothesis that Ea/p apical constriction drives the movement of the MSxx cells, suggesting that MSxx cell polarity is not important for the bulk of MSxx cell movement (Lee and Goldstein, 2003). However, it is possible that the MSxx cells are motile without surface retrograde flow. There is evidence that some cells can produce lamellipodial protrusions and move by rolling, without retrograde flow (Anderson et al., 1996). Additionally, although the cell manipulation experiments suggest that MSxx cell crawling is not a significant component of normal MSxx cell movement, it is possible that reoriented cells become re-polarized upon reassociation. Therefore, we do not yet know whether the F-actin-rich structures are specializations for cell motility.

There are a number of precedents for the formation of F-actin-rich structures in cells during morphogenesis. For example, F-actin-rich filopodial extensions form during *C. elegans* ventral enclosure (Williams-Masson et al., 1997). In addition to proposed roles for filopodia in cell motility during ventral enclosure, these actin-rich fingers might have a role in cell-cell adhesion (Raich et al., 1999). In a process termed ‘filopodial priming’, α-catenin is rapidly recruited at sites where contralateral filopodial tips first make contact. This recruitment is thought to allow for rapid cell-cell

adhesion as the epithelium seals on the ventral side. Our experiments suggest that proper cell fate is required for the formation of these F-actin-rich structures. Interestingly, although the transformation of MS cells to E cells resulted in the internalization of both groups of cells, we did not observe the formation of F-actin-rich structures on the border of MS and E cells. However, we also never observed complete internalization of Ea/p cells. Whether the F-actin-rich processes on the MSxx cells function similarly to how they function in ventral enclosure to seal the ventral opening during gastrulation is not yet known. However, it is possible that the extensions might function in sealing a gap given the localization of the extensions, on one side of a closing gap.

The combination of actomyosin contractility in internalizing cells with F-actin nucleation in their neighbors in *C. elegans* gastrulation is similar to what is observed in zebrafish gastrulation (Lai et al., 2008). In this system, Rho signaling regulates actomyosin contractility and neighboring cell migration, controlling cell movements during epiboly and convergent extension. A diaphanous-related formin is required for filopodial-like processes to form in marginal deep cells. Perhaps Arp2/3 is acting redundantly with other actin-nucleating proteins in *C. elegans*. If *C. elegans* Arp2/3 were depleted together with other F-actin regulating proteins, such as formins, further defects might occur during Ea/p cell internalization. However, the formins have a role in cytokinesis throughout earlier embryogenesis (Swan et al., 1998), precluding us from carrying out simple double-knockdown experiments.

In Arp2/3 RNAi embryos, the F-actin-rich structures that we have detailed do not form. Our Arp2/3 immunostaining studies indicate that Arp2/3 localizes to the cell cortex at the time of Ea/p cell internalization, including at the boundary between MSxx cells and the Ea cell. However, whether the absence of the F-actin structures in Arp2/3 RNAi embryos is due to a direct role for Arp2/3 in the formation of these structures, or whether it is a secondary effect of plasma membrane dissociation from the cell cortex as in blebs, is currently unknown. The Ea/p cell internalization defect seen in Arp2/3 RNAi embryos could also be due in part to defective actin organization in the apically constricting Ea/p cells, independent of the role of Arp2/3 in the MS cells. Myosin-II remains apically localized and activated in Arp2/3 RNAi embryos, but the architecture of the actin network in the apical cortex of the Ea/p cells might be disorganized in ways that are not obvious at the resolution limit of the confocal or spinning disk confocal imaging used (estimated to be about 200 nm). Such disorganization could affect the ability of myosin-II to contract the apical actin network.

Because the F-actin-rich extensions we observed formed only on MS-derived cells and not on other members of the ring of six cells, and because they formed only on the three MS-derived cells that contacted Ea/p, we speculate that the structures might be induced in MS progeny by signals or physical cues from Ea/p. Our observation that the apical protein PAR-3 is required for the formation of MSxx-specific extensions suggests that apicobasal cell polarity has a role, either direct or indirect, in spatially regulating F-actin distribution. We do not know whether the absence of MSxx extensions reflects a role for PAR-3 in the Ea/p cells, in the MSxx cells or both. Apicobasal polarity in the Ea/p cells could be important for the Ea/p cells to produce a hypothetical signal to the MSxx cells to form the extensions. The formation of the extensions could also require the normal behavior of internalizing Ea/p cells to produce an effective physical cue. We found that Arp2/3 cortical localization was preserved in *par-3 ZF1* mutants. This was expected, given that actin localization as observed by GFP::MOE was also cortical. We also found that Arp2/3 localized to the boundary between MS granddaughters and Ea/p cells in *par-3 ZF1* mutants, although F-actin-rich structures did not form. This suggests that Arp2/3 localization is not sufficient to induce the formation of the extensions, and it provides further evidence that the lack of F-actin-rich extensions in Arp2/3-depleted embryos might be an indirect effect of actin architecture misregulation, and perhaps a result of loss of cortical integrity.

We have shown that the blebs observed in Arp2/3 RNAi embryos (Severson et al., 2002) involve plasma membrane dissociation from the cell cortex. During bleb formation, the plasma membrane protruded without an F-actin-rich cortex. Once bleb growth stopped, GFP::MOE assembled underneath the plasma membrane at the bleb, and the bleb retracted. These dynamics are similar to those seen in human cell lines (Charras et al., 2006). However, there are some differences. In human cells, membrane blebs expanded for 5-7 seconds, and remained in a fully expanded state for about 30 seconds. Once F-actin and other contractile machinery assembled under the membrane blebs, retraction occurred slowly, over the course of one minute (Charras et al., 2006). In Arp2/3 RNAi *C. elegans* embryos, the blebs appeared and disappeared all within 30 seconds, and the rate of retraction did not appear to be slower than the rate of expansion. We do not know whether these differences in dynamics reflect differences between systems or differences between normal and Arp2/3-deficient bleb formation. In human cells, membrane blebs can form as a result of detachment of the membrane from the cytoskeleton (Charras et al., 2006). However, ruptures in the cell cortex can also lead to dissociation of the membrane with the cortex, and the flow of cytoplasm into the area results in formation of a membrane bleb (Paluch et al., 2005; Paluch et al., 2006; Sheetz and Dai, 1996). Since Arp2/3 is a major actin regulator, it is likely that the membrane blebs that form in Arp2/3-depleted embryos are a result of loss of microfilament density and the formation of ruptures in the cortex. Indeed, we see little F-actin beneath growing blebs (Fig. 3I,J).

Given the pronounced blebbing at free surfaces in Arp2/3 RNAi embryos, we were surprised that many features of the Ea/p cells were normal. Our results suggest that cell fate, PAR protein localization, and myosin localization and activation are not affected by any global changes of the actin cytoskeleton that occur in the absence of Arp2/3, including formation of membrane blebs. The normal apicobasal polarization we observed of PAR proteins and myosin-II suggests that any role that Arp2/3 might have in vesicle trafficking in this system must not be essential to regulate localization of these proteins. It is possible that PAR proteins and myosin-II are localized by other mechanisms, or by Arp2/3-independent vesicle trafficking.

The most well-characterized role of Arp2/3 is as a regulator of the branched actin network in migrating epithelial cells and growth cones in culture (Pollard, 2007). Additionally, Arp2/3 has been shown to have many roles during morphogenesis, mostly ascribable to its role in regulating actin architecture (Vartiainen and Machesky, 2004). However, almost all of the previously described roles of Arp2/3 in morphogenesis were in non-moving cells. Therefore, we sought to bridge what is known about Arp2/3 in tissue culture studies with morphogenesis in developmental systems, to establish roles for Arp2/3 in moving cells during morphogenesis. Our results identify specific cellular roles for Arp2/3 in an embryo during morphogenesis. The results also add a layer to our pre-existing model of *C. elegans* gastrulation. In addition to apical constriction,

internalization of the endoderm might involve dynamic, Arp2/3-dependent, F-actin-rich extensions on one side of a closing ring of cells.

Materials and Methods

Strains and worm maintenance

Nematodes were cultured and handled as described (Brenner, 1974). Unless indicated, experiments were performed with the wild-type N2 (Bristol) strain. The following mutant and reporter strains were used: KK866 GFP::PAR-2, JJ1473 *unc-119 (ed3)* III; *zuIs45* [*nmy-2*::NMY-2::GFP; *unc-119 (+)*]; referred to here as NMY-2::GFP, JJ1317 *zuIs3* [*end-1*::GFP], OD70 *ltIs44* [*pie-1*::PH domain of PLCγ::mCherry] (PH::mCherry) (Kachur et al., 2008), PF100 nnIs [*u*nc-119(+) pie-1 *promoter::*gfp::*Dm-moesin*$^{437–578}$ (amino acids 437–578 of *D. melanogaster* Moesin)] (GFP::MOE), *unc-32(e189) par-3(it71); zuIs20*(*par-3*::PAR-3;ZF1-GFP) (PAR-3-ZF1) (a gift from Jeremy Nance, Skirball Institute, NY), LP53 PH::mCherry; GFP::MOE, MS632 *unc-119(ed4)* III; *irIs39* [*ced-51*::NLS::GFP] (Broitman-Maduro et al., 2009), LP54 PH::mCherry; NMY-2::GFP. LP53 and LP54 were constructed by crossing OD70 PH::mCherry males with PF100 GFP::MOE or JJ1473 NMY-2::GFP hermaphrodites, respectively. All strains were maintained at 20°C, except for the following strains: KK866 PAR-2::GFP, PF100 GFP::MOE, JJ1473 NMY-2::GFP, LP53 PH::mCherry; GFP::MOE, and LP54 PH::mCherry; NMY-2::GFP were maintained at 24°C. Imaging was performed at 20°C–23°C for all strains.

DIC and confocal time-lapse microscopy

Embryos were mounted and DIC images were acquired as described (McCarthy Campbell et al., 2009). Time-lapse images were acquired at 1 μm optical sections every 1 minute and analyzed with Metamorph software (Molecular Devices). Gastrulation was scored by examination of whether the Ea and Ep cells were completely surrounded by neighboring cells in three dimensions at the time that Ea and Ep divided. If Ea and Ep divided before being completely surrounded, we scored gastrulation as having failed. For measuring apical membranes, the length of the ventral surface was measured in the optical section in which this length was greatest, from the Ea-Ep ventral border to both the Ep-P_4 ventral border and the Ea-MSxx ventral border. Spinning disk confocal images were acquired and processed as described (Lee et al., 2006). To observe the apical boundaries of Ea/p cells during internalization, we filmed the ventral surface of PH::mCherry embryos. Three 2 μm steps were taken every 5 seconds to capture the entire apical surface of the Ea/p cell. To analyze GFP::MOE dynamics, a single plane was acquired every 5 seconds once MSxx cells were born.

RNA interference

RNAi by injection was performed according to a standard protocol (Dudley et al., 2002), except that a cDNA preparation was used as template to PCR *arx* genes. *arx-1/Arp3* and *arx-2/Arp2* specific primers were used to amplify the entire open reading frame (approximately 1 kb). Double-stranded RNA was injected at a concentration of 100 ng/ml. Embryos were analyzed 22-25 hours later.

Analysis of NMY-2::GFP accumulation

NMY-2::GFP and Arp2/3 (RNAi); NMY-2::GFP embryos were imaged on a spinning disk confocal microscope as above. Images were captured once each minute after MSa/p division. To analyze NMY-2::GFP levels, a line was first drawn perpendicular to the Ea/p cell cortex. With Metamorph software, these lines were converted into kymographs of maximum pixel intensity over time. NMY-2::GFP levels were quantified by calculating the ratio of cortical to cytoplasmic fluorescence intensities (pixel intensity levels above off-embryo background).

Analysis of cortical blebs

GFP::MOE; PH::mCherry embryos were imaged on a spinning disk confocal microscope as above. Single plane images for each of GFP::MOE and PH::mCherry were taken every 3 seconds. Perpendicular linescans were drawn through the membrane blebs with Metamorph software and converted to kymographs.

Analysis of GFP::MOE distribution

GFP::MOE, Arp2/3 (RNAi); GFP::MOE, and *par-3* ZF1; GFP::MOE embryos were imaged on their ventral surfaces on a spinning disk confocal microscope as above. Images were captured once every three seconds generally starting six minutes after MSa/p cell division. To analyze GFP::MOE levels, a three by three pixel low pass filter was applied, and a line was then drawn along the long axis of each MSxx cell. Lines were converted into kymographs of maximum pixel intensity over time using Metamorph. Linescans along the front and rear MSxx cell boundaries in the kymograph were plotted, and ratios of the GFP::MOE fluorescence intensity between the cell boundaries were determined. These ratios were converted to 5-timepoint running average heatmaps with colors representing a two-fold higher (yellow) or two-fold lower (blue) difference in GFP::MOE concentration at the front cell boundary as compared to the back using a custom-written BASIC program. Rare ratios beyond two-fold were represented as two-fold.

Immunostaining and confocal microscopy

ARX-5 polyclonal antibodies were generated from rabbits expressing the polypeptide KFDTELKVLPLGNTNMGKLPIRTNFKGPAPQTNQDDIIDEALTYFKPNIFFREF-EIKGPADRTMIYLIFYITECLRKLQKSPNKIAGQKDLHALALSHLL (Strategic Diagnostics). Antiserum was affinity purified to an endpoint titer of 0.35 ng/ml. Immunostaining of embryos for p-rMLC (Abcam) was performed according to previously described protocols (Lee et al., 2006; Marston et al., 2008). Immunostaining embryos for GFP (for PAR-2::GFP) (1:100, Invitrogen), PAR-3 (1:100, Developmental Studies Hybridoma Bank), ARX-5 (1:1000, Strategic Diagnostics), and OIC1D4 for P granules (1:200, Developmental Studies Hybridoma Bank) was performed as described (Tenlen et al., 2008). PAR-2::GFP and anti-PAR-3 fluorescence intensity were measured by recording linescans across the Ea/p cell apical and basolateral membranes using Metamorph software. For PAR-3, the Ea/p cell basolateral membrane was identified by determining the localization border of an E-cell specific marker, *end-1*::GFP. Levels were calculated as three-pixel running averages in each embryo, and apical and basolateral peaks were used to align measurements between embryos.

We thank Anjon Audhya, Morris Maduro, Jeremy Nance and the Caenorhabditis Genetics Center for strains; Brent Hehl for constructing a strain; and Steve Rogers and members of our lab for discussion and comments. This work was supported by National Institutes of Health RO1-GM083071 to B.G. Deposited in PMC for release after 12 months.

References

Anderson, K. I., Wang, Y. L. and Small, J. V. (1996). Coordination of protrusion and translocation of the keratocyte involves rolling of the cell body. *J. Cell Biol.* **134**, 1209-1218.

Boyd, L., Guo, S., Levitan, D., Stinchcomb, D. T. and Kemphues, K. J. (1996). PAR-2 is asymmetrically distributed and promotes association of P granules and PAR-1 with the cortex in C. elegans embryos. *Development* **122**, 3075-3084.

Brenner, S. (1974). The genetics of Caenorhabditis elegans. *Genetics* **77**, 71-94.

Broitman-Maduro, G., Owraghi, M., Hung, W. W., Kuntz, S., Sternberg, P. W. and Maduro, M. F. (2009). The NK-2 class homeodomain factor CEH-51 and the T-box factor TBX-35 have overlapping function in C. elegans mesoderm development. *Development* **136**, 2735-2746.

Calvo, D., Victor, M., Gay, F., Sui, G., Luke, M. P., Dufourcq, P., Wen, G., Maduro, M., Rothman, J. and Shi, Y. (2001). A POP-1 repressor complex restricts inappropriate cell type-specific gene transcription during Caenorhabditis elegans embryogenesis. *EMBO J.* **20**, 7197-7208.

Charras, G. T., Hu, C. K., Coughlin, M. and Mitchison, T. J. (2006). Reassembly of contractile actin cortex in cell blebs. *J. Cell Biol.* **175**, 477-490.

Cunningham, C. C. (1995). Actin polymerization and intracellular solvent flow in cell surface blebbing. *J. Cell Biol.* **129**, 1589-1599.

Dudley, N. R., Labbe, J. C. and Goldstein, B. (2002). Using RNA interference to identify genes required for RNA interference. *Proc. Natl. Acad. Sci. USA* **99**, 4191-4196.

Edgar, L. G. and McGhee, J. D. (1988). DNA synthesis and the control of embryonic gene expression in C. elegans. *Cell* **53**, 589-599.

Edwards, K. A., Demsky, M., Montague, R. A., Weymouth, N. and Kiehart, D. P. (1997). GFP-moesin illuminates actin cytoskeleton dynamics in living tissue and demonstrates cell shape changes during morphogenesis in Drosophila. *Dev. Biol.* **191**, 103-117.

Etemad-Moghadam, B., Guo, S. and Kemphues, K. J. (1995). Asymmetrically distributed PAR-3 protein contributes to cell polarity and spindle alignment in early C. elegans embryos. *Cell* **83**, 743-752.

Fucini, R. V., Chen, J. L., Sharma, C., Kessels, M. M. and Stamnes, M. (2002). Golgi vesicle proteins are linked to the assembly of an actin complex defined by mAbp1. *Mol. Biol. Cell* **13**, 621-631.

Galletta, B. J. and Cooper, J. A. (2009). Actin and endocytosis: mechanisms and phylogeny. *Curr. Opin. Cell Biol.* **21**, 20-27.

Georgiou, M., Marinari, E., Burden, J. and Baum, B. (2008). Cdc42, Par6, and aPKC regulate Arp2/3-mediated endocytosis to control local adherens junction stability. *Curr. Biol.* **18**, 1631-1638.

Goldstein, B. (2000). When cells tell their neighbors which direction to divide. *Dev. Dyn.* **218**, 23-29.

Goldstein, B. and Macara, I. G. (2007). The PAR proteins: fundamental players in animal cell polarization. *Dev. Cell* **13**, 609-622.

Guerriero, C. J., Weixel, K. M., Bruns, J. R. and Weisz, O. A. (2006). Phosphatidylinositol 5-kinase stimulates apical biosynthetic delivery via an Arp2/3-dependent mechanism. *J. Biol. Chem.* **281**, 15376-15384.

Hudson, A. M. and Cooley, L. (2002). A subset of dynamic actin rearrangements in Drosophila requires the Arp2/3 complex. *J. Cell Biol.* **156**, 677-687.

Hung, T. J. and Kemphues, K. J. (1999). PAR-6 is a conserved PDZ domain-containing protein that colocalizes with PAR-3 in Caenorhabditis elegans embryos. *Development* **126**, 127-135.

Kachur, T. M., Audhya, A. and Pilgrim, D. B. (2008). UNC-45 is required for NMY-2 contractile function in early embryonic polarity establishment and germline cellularization in C. elegans. *Dev. Biol.* **314**, 287-299.

Kovacs, E. M. and Yap, A. S. (2002). The web and the rock: cell adhesion and the ARP2/3 complex. *Dev. Cell* **3**, 760-761.

Lai, S. L., Chan, T. H., Lin, M. J., Huang, W. P., Lou, S. W. and Lee, S. J. (2008). Diaphanous-related formin 2 and profilin I are required for gastrulation cell movements. *PLoS One* **3**, e3439.
Le Clainche, C. and Carlier, M. F. (2008). Regulation of actin assembly associated with protrusion and adhesion in cell migration. *Physiol. Rev.* **88**, 489-513.
Lee, J. Y. and Goldstein, B. (2003). Mechanisms of cell positioning during C. elegans gastrulation. *Development* **130**, 307-320.
Lee, J. Y., Marston, D. J., Walston, T., Hardin, J., Halberstadt, A. and Goldstein, B. (2006). Wnt/Frizzled signaling controls C. elegans gastrulation by activating actomyosin contractility. *Curr. Biol.* **16**, 1986-1997.
Lin, R., Thompson, S. and Priess, J. R. (1995). pop-1 encodes an HMG box protein required for the specification of a mesoderm precursor in early C. elegans embryos. *Cell* **83**, 599-609.
Luna, A., Matas, O. B., Martinez-Menarguez, J. A., Mato, E., Duran, J. M., Ballesta, J., Way, M. and Egea, G. (2002). Regulation of protein transport from the Golgi complex to the endoplasmic reticulum by CDC42 and N-WASP. *Mol. Biol. Cell* **13**, 866-879.
Maduro, M. F., Hill, R. J., Heid, P. J., Newman-Smith, E. D., Zhu, J., Priess, J. R. and Rothman, J. H. (2005). Genetic redundancy in endoderm specification within the genus Caenorhabditis. *Dev. Biol.* **284**, 509-522.
Marston, D. J., Roh, M., Mikels, A. J., Nusse, R. and Goldstein, B. (2008). Wnt signaling during Caenorhabditis elegans embryonic development. *Methods Mol. Biol.* **469**, 103-111.
Massarwa, R., Carmon, S., Shilo, B. Z. and Schejter, E. D. (2007). WIP/WASp-based actin-polymerization machinery is essential for myoblast fusion in Drosophila. *Dev. Cell.* **12**, 557-569.
Mathur, J. (2005). The ARP2/3 complex: giving plant cells a leading edge. *BioEssays* **27**, 377-387.
May, R. C., Caron, E., Hall, A. and Machesky, L. M. (2000). Involvement of the Arp2/3 complex in phagocytosis mediated by FcgammaR or CR3. *Nat. Cell Biol.* **2**, 246-248.
McCarthy Campbell, E. K., Werts, A. D. and Goldstein, B. (2009). A cell cycle timer for asymmetric spindle positioning. *PLoS Biol.* **7**, e1000088.
Motegi, F., Velarde, N. V., Piano, F. and Sugimoto, A. (2006). Two phases of astral microtubule activity during cytokinesis in C. elegans embryos. *Dev. Cell* **10**, 509-520.
Mullins, R. D., Stafford, W. F. and Pollard, T. D. (1997). Structure, subunit topology, and actin-binding activity of the Arp2/3 complex from Acanthamoeba. *J. Cell Biol.* **136**, 331-343.
Nance, J. and Priess, J. R. (2002). Cell polarity and gastrulation in C. elegans. *Development* **129**, 387-397.
Nance, J., Munro, E. M. and Priess, J. R. (2003). C. elegans PAR-3 and PAR-6 are required for apicobasal asymmetries associated with cell adhesion and gastrulation. *Development* **130**, 5339-5350.
Paluch, E., Piel, M., Prost, J., Bornens, M. and Sykes, C. (2005). Cortical actomyosin breakage triggers shape oscillations in cells and cell fragments. *Biophys. J.* **89**, 724-733.
Paluch, E., Sykes, C., Prost, J. and Bornens, M. (2006). Dynamic modes of the cortical actomyosin gel during cell locomotion and division. *Trends Cell Biol.* **16**, 5-10.
Patel, F. B., Bernadskaya, Y. Y., Chen, E., Jobanputra, A., Pooladi, Z., Freeman, K. L., Gally, C., Mohler, W. A. and Soto, M. C. (2008). The WAVE/SCAR complex promotes polarized cell movements and actin enrichment in epithelia during C. elegans embryogenesis. *Dev. Biol.* **324**, 297-309.
Pollard, T. D. (2007). Regulation of actin filament assembly by Arp2/3 complex and formins. *Annu. Rev. Biophys. Biomol. Struct.* **36**, 451-477.
Pollard, T. D. and Borisy, G. G. (2003). Cellular motility driven by assembly and disassembly of actin filaments. *Cell* **112**, 453-465.
Raich, W. B., Agbunag, C. and Hardin, J. (1999). Rapid epithelial-sheet sealing in the Caenorhabditis elegans embryo requires cadherin-dependent filopodial priming. *Curr. Biol.* **9**, 1139-1146.
Rouiller, I., Xu, X. P., Amann, K. J., Egile, C., Nickell, S., Nicastro, D., Li, R., Pollard, T. D., Volkmann, N. and Hanein, D. (2008). The structural basis of actin filament branching by the Arp2/3 complex. *J. Cell Biol.* **180**, 887-895.
Sawa, M., Suetsugu, S., Sugimoto, A., Miki, H., Yamamoto, M. and Takenawa, T. (2003). Essential role of the C. elegans Arp2/3 complex in cell migration during ventral enclosure. *J. Cell Sci.* **116**, 1505-1518.
Schmidt, K. L., Marcus-Gueret, N., Adeleye, A., Webber, J., Baillie, D. and Stringham, E. G. (2009). The cell migration molecule UNC-53/NAV2 is linked to the ARP2/3 complex by ABI-1. *Development* **136**, 563-574.
Severson, A. F., Baillie, D. L. and Bowerman, B. (2002). A Formin Homology protein and a profilin are required for cytokinesis and Arp2/3-independent assembly of cortical microfilaments in C. elegans. *Curr. Biol.* **12**, 2066-2075.
Sheetz, M. P. and Dai, J. (1996). Modulation of membrane dynamics and cell motility by membrane tension. *Trends Cell Biol.* **6**, 85-89.
Somogyi, K. and Rorth, P. (2004). Cortactin modulates cell migration and ring canal morphogenesis during Drosophila oogenesis. *Mech. Dev.* **121**, 57-64.
Stevenson, V., Hudson, A., Cooley, L. and Theurkauf, W. E. (2002). Arp2/3-dependent pseudocleavage [correction of psuedocleavage] furrow assembly in syncytial Drosophila embryos. *Curr. Biol.* **12**, 705-711.
Svitkina, T. M. and Borisy, G. G. (1999). Arp2/3 complex and actin depolymerizing factor/cofilin in dendritic organization and treadmilling of actin filament array in lamellipodia. *J. Cell Biol.* **145**, 1009-1026.
Swan, K. A., Severson, A. F., Carter, J. C., Martin, P. R., Schnabel, H., Schnabel, R. and Bowerman, B. (1998). cyk-1: a C. elegans FH gene required for a late step in embryonic cytokinesis. *J. Cell Sci.* **111**, 2017-2027.
Takizawa, P. A., Sil, A., Swedlow, J. R., Herskowitz, I. and Vale, R. D. (1997). Actin-dependent localization of an RNA encoding a cell-fate determinant in yeast. *Nature* **389**, 90-93.
Tenlen, J. R., Molk, J. N., London, N., Page, B. D. and Priess, J. R. (2008). MEX-5 asymmetry in one-cell C. elegans embryos requires PAR-4- and PAR-1-dependent phosphorylation. *Development* **135**, 3665-3675.
Vartiainen, M. K. and Machesky, L. M. (2004). The WASP-Arp2/3 pathway: genetic insights. *Curr. Opin. Cell Biol.* **16**, 174-181.
Warren, D. T., Andrews, P. D., Gourlay, C. W. and Ayscough, K. R. (2002). Sla1p couples the yeast endocytic machinery to proteins regulating actin dynamics. *J. Cell Sci.* **115**, 1703-1715.
Williams-Masson, E. M., Malik, A. N. and Hardin, J. (1997). An actin-mediated two-step mechanism is required for ventral enclosure of the C. elegans hypodermis. *Development* **124**, 2889-2901.
Zhu, J., Hill, R. J., Heid, P. J., Fukuyama, M., Sugimoto, A., Priess, J. R. and Rothman, J. H. (1997). end-1 encodes an apparent GATA factor that specifies the endoderm precursor in Caenorhabditis elegans embryos. *Genes Dev.* **11**, 2883-2896.

Journal of Cell Science